

Surface and Interfacial Passivations for FASnI_3 Solar Cells with Co-Cations

Chun-Hsiao Kuan, Yu-An Ko, and Eric Wei-Guang Diau*

Cite This: *ACS Energy Lett.* 2023, 8, 2423–2425

Read Online

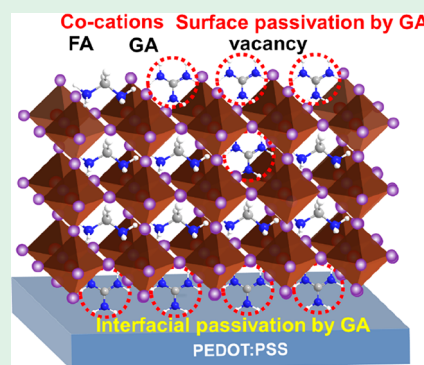
ACCESS |

Metrics & More

Article Recommendations

Supporting Information

ABSTRACT: Seven cations, methylammonium (MA), ethylammonium (EA), aziridinium (AZ), dimethylammonium (DMA), 2-hydroxyethylammonium (HEA), imidazolium (IM), and guanidinium (GA), were used to cocrystallize with formamidinium (FA) to form cationic tin perovskite solar cells (TPSCs) using a two-step fabrication procedure. Time-of-flight second ion mass spectrometry results indicate that the pristine FA-based TPSC involved both vacancies on the perovskite surface and perovskite/poly(3,4-ethylenedioxythiophene):poly(styrenesulfonate) (PEDOT:PSS) interface, and GA has the ability to passivate both surface and interfacial vacancy defects to give impressive device performance (PCE = 11.2%) and stability (>5000 h) with a negligible effect of hysteresis.



Perovskite solar cells (PSCs) attract much attention as a new alternative for next-generation photovoltaic applications.^{1–5} However, PSCs contain the toxic lead that should be replaced with a nontoxic element such as tin.⁵ As a result, tin-based PSCs (TPSCs) emerged to be one of the most promising candidates for lead-free perovskite solar cells.⁵ The intrinsic problems for TPSCs are $\text{Sn}^{2+}/\text{Sn}^{4+}$ oxidation, rapid crystallization, poor enduring stability, and so on, which should be solved to further promote the device performance for TPSCs.⁶ Many additives have been applied to tackle these problems.^{7,8} Presently, tin fluoride (SnF_2) and ethylene diammonium diiodide (EDAI_2) are the two most common additives used for formamidinium (FA)-based TPSCs.⁹ In addition to these two additives, other cationic additives have been widely considered for TPSCs. For example, methylammonium (MA),¹⁰ ethylammonium (EA),¹¹ 2-hydroxyethylammonium (HEA),¹² dimethylammonium (DMA),¹³ aziridinium (AZ),¹⁴ imidazolium (IM),¹⁵ guanidinium (GA),¹⁶ and so on have been applied as A-site cations to cocrystallize with FA to form cationic tin perovskites for enhanced performance and stability for TPSCs. These cationic approaches were performed according to a one-step fabrication procedure for which all tin perovskite precursors were added together in a solution to deposit on the hole-transport layer poly(3,4-ethylenedioxythiophene):poly(styrenesulfonate) (PEDOT:PSS) in one step. However, the reaction between SnI_2 and FAI/AI (A represents a cation) was very rapid so that a two-step fabrication approach is favorable to retard the crystal growth rate.^{17,18} We have recently demonstrated the application using the two-step method to deposit tin perovskite film on

varied hole-transporting material (HTM) and self-assemble monolayer (SAM) surfaces with good device performance and stability.^{19–22} In the present study, we systematically investigate a series of organic cations, MA, EA, AZ, DMA, HEA, IM, and GA (Figure 1a) on the A-site position to form cocations with FA in a $\text{FA}_x\text{A}_{1-x}\text{SnI}_3$ (FA/A) solar cell using the two-step fabrication method in the presence of 20% SnF_2 and 1% EDAI_2 . The data of the top-view SEM (Figure S1), AFM (Figure S2), side-view SEM (Figure S3), XRD (Figure S4), UV–vis/PL spectra (Figure S5), UPS (Figure S6), TCSPC (Figure S7), EIS (Figure S8), GIWAXS (Figure S9), energy level diagram (Figure S10), and TOF-SIMS (Figure 2) are shown to help with understanding of the device performance in relation to morphology, crystallinity, and optical and optoelectronic properties of this cationic system. We found that the FA/GA device exhibited the best performance with a PCE of 11.2%, which is a record performance for TPSC fabricated using a two-step approach. Surface passivation on both sides of the perovskite layer plays an important role to attain such a great device performance and stability.

The devices were fabricated in a structure of ITO/PEDOT:PSS/perovskite/C60/BCP/Ag for the perovskite active layer made of pure ASnI_3 with a two-step method,

Received: April 7, 2023

Accepted: April 26, 2023

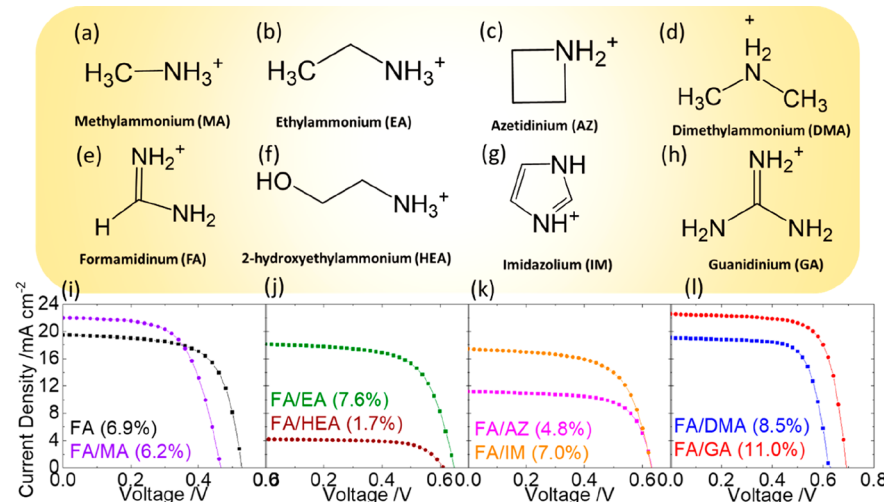


Figure 1. Chemical structures of different cations for (a) MA, (b) EA, (c) AZ, (d) DMA, (e) FA, (f) HEA, (g) IM, and (h) GA. The corresponding device performances obtained from reverse J – V scans are shown underneath for (i) FA and FA/MA, (j) FA/EA and FA/HEA, (k) FA/AZ and FA/IM, and (l) FA/DMA and FA/GA.

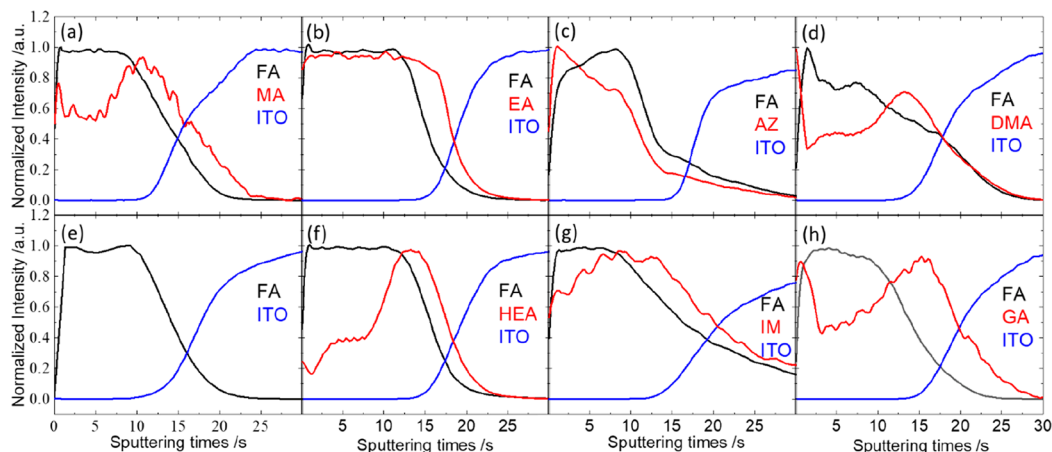


Figure 2. TOF-SIMS depth profiles for the cationic films made of (a) FA/MA, (b) FA/EA, (c) FA/AZ, (d) FA/DMA (e) pristine FA, (f) FA/HEA, (g) FA/IM, and (h) FA/GA.

where A is the eight organic cations shown in Figure 1. As expected, the FASnI_3 device outperformed the other devices as the J – V characteristics show in Figure S11. Therefore, FA was selected as a core cation to cocrystallize with the other seven cations shown in Figure 1. For the $\text{FA}_x\text{A}_{1-x}\text{SnI}_3$ device, we fixed the FA/A ratio according to the condition of the optimized FA/GA device (Figure S12). As shown in Figure 1i–l, the devices made of FA/A cations show the performances with the order FA/GA (11.0%) > FA/DMA (8.5%) > FA/EA (7.6%) > FA/IM (7.0%) > pristine FA (6.9%) > FA/MA (6.3%) > FA/AZ (4.8%) > FA/HEA (1.7%). The device performances are consistent with the morphological features (Figure S1) with larger and uniformed crystals in the FA/GA and FA/DMA films, and with poorer morphologies and pin holes in the FA/AZ and FA/HEA films. As a champion device, the FA/GA film also exhibited smaller roughness (Figure S2) with a greater film thickness (Figure S3), longer PL lifetime (Figure S7), greater crystallinity (Figures S4 and S9), and larger recombination resistance (Figure S8) than the others. The device performance of FA/GA with a two-step method is much greater than our previous report using 20% of GA in FASnI_3 according to a conventional one-step fabrication method (11.0% vs 9.6%).¹⁶

To understand the distribution of the cations in the FA/A films, we performed TOF-SIMS investigations for all films; the corresponding results are shown in Figure 2. The TOF-SIMS data of the pristine FA film show a flat feature in the bulk region but with vacancy defects on the perovskite surface and FA/HTM interface. The FA/AZ film lacks both interfacial and surface defect passivations so that it did not show good device performance. The FA/MA, FA/IM, and FA/HEA films have interfacial defect passivation but without surface passivation to obtain good device performance. The FA/EA film has both FA and EA cations distributed evenly throughout the perovskite film so that it gives a moderate device performance. For the DMA film, the FA and DMA cation distributions reflect a mirror image to each other, indicating that DMA can passivate both surface and interfacial defects to give a decent device performance. For the GA film, the FA distribution is flat in the bulk region, which indicates that a good crystallinity may be involved. However, certain vacancy defects existed on the perovskite surface and in the FA/HTM interfacial region. GA thus plays a key role to effectively passivate both surface and interfacial defects to give excellent device performance with great shelf-storage stability over 5000 h without degradation of the device performance

(Figure S13), which is a remarkable record for a PEDOT:PSS-based TPSC. Note that GA is a nonpolar cation, the interfacial passivation via GA thus significantly enhances the stability of the FA/GA device. Furthermore, negligible hysteresis was observed for the FA/GA device (Figure S14), for which a forward scan gave a lightly higher PCE of 11.2%. In conclusion, the hybrid FA/GA device was studied to provide excellent performance and stability due to the great passivation capability of GA to passivate both surface and interfacial FA vacancy defects.

■ ASSOCIATED CONTENT

§ Supporting Information

The Supporting Information is available free of charge at <https://pubs.acs.org/doi/10.1021/acsenergylett.3c00742>.

Description of supplementary text; experimental details; supplemental Figures S1–S13 ([PDF](#))

■ AUTHOR INFORMATION

Corresponding Author

Eric Wei-Guang Diau – Department of Applied Chemistry and Institute of Molecular Science and Center for Emergent Functional Matter Science, National Yang Ming Chiao Tung University, Hsinchu 300093, Taiwan;  orcid.org/0000-0001-6113-5679; Email: diau@nycu.edu.tw

Authors

Chun-Hsiao Kuan – Department of Applied Chemistry and Institute of Molecular Science, National Yang Ming Chiao Tung University, Hsinchu 300093, Taiwan

Yu-An Ko – Department of Applied Chemistry and Institute of Molecular Science, National Yang Ming Chiao Tung University, Hsinchu 300093, Taiwan

Complete contact information is available at:

<https://pubs.acs.org/10.1021/acsenergylett.3c00742>

Notes

The authors declare no competing financial interest.

■ ACKNOWLEDGMENTS

We thank Mr. Chiung-Chi Wang (Instrumentation Center, NTHU) for the assistance on TOF-SIMS measurements. We thank Prof. C.-S. Lin and Ms. Y.-T. Lee of Instrumentation Center, National Taiwan University for FEG-SEM experiments. We also thank Dr. Y.-W. Tsai and Dr. J.-M. Lin (TPS 25A1 NSRRC) for their kind assistance in GIWAXS data analysis. This work is supported by the National Science and Technology Council (NSTC), Taiwan (grant no. NSTC 111-2634-F-A49-007 and NSTC 111-2123-M-A49-001) and the Center for Emergent Functional Matter Science of National Yang Ming Chiao Tung University (NYCU) from The Featured Areas Research Center Program within the framework of the Higher Education Sprout Project by the Ministry of Education (MOE) in Taiwan.

■ REFERENCES

- (1) Jiang, Q.; et al. Compositional Texture Engineering for Highly Stable Wide-bandgap Perovskite Solar Cells. *Science* **2022**, *378* (6626), 1295–1300.
- (2) Jiang, Q.; et al. Surface Reaction for Efficient and Stable Inverted Perovskite Solar Cells. *Nature* **2022**, *611* (7935), 278–283.
- (3) Ma, W.; et al. Thermally Activated Delayed Fluorescence (TADF) Organic Molecules for Efficient X-ray Scintillation and Imaging. *Nat. Mater.* **2022**, *21* (2), 210–216.
- (4) Diau, E. W.-G. Next-generation Solar Cells and Conversion of Solar Energy. *ACS Energy Lett.* **2017**, *2* (2), 334–335.
- (5) Diau, E. W.-G.; Jokar, E.; Rameez, M. Strategies to Improve Performance and Stability for Tin-based Perovskite Solar Cells. *ACS Energy Lett.* **2019**, *4* (8), 1930–1937.
- (6) Yu, B. B.; et al. Heterogeneous 2D/3D Tin-halides Perovskite Solar Cells with Certified Conversion Efficiency Breaking 14%. *Adv. Mater.* **2021**, *33* (36), 2102055.
- (7) Jokar, E.; et al. Slow Passivation and Inverted Hysteresis for Hybrid Tin Perovskite Solar Cells Attaining 13.5% Via Sequential Deposition. *J. Phys. Chem. Lett.* **2021**, *12* (41), 10106–10111.
- (8) Jokar, E.; et al. Enhanced Performance and Stability of 3D/2D Tin Perovskite Solar Cells Fabricated with A Sequential Solution Deposition. *ACS Energy Lett.* **2021**, *6* (2), 485–492.
- (9) Jokar, E.; et al. Slow Surface Passivation and Crystal Relaxation with Additives to Improve Device Performance and Durability for Tin-based Perovskite Solar Cells. *Energy Environ. Sci.* **2018**, *11* (9), 2353–2362.
- (10) Li, F.; et al. FA/MA Cation Exchange for Efficient and Reproducible Tin-based Perovskite Solar Cells. *ACS Appl. Mater. Interfaces* **2021**, *13* (34), 40656–40663.
- (11) Nishimura, K.; et al. Lead-free Tin-halide Perovskite Solar Cells with 13% Efficiency. *Nano Energy* **2020**, *74*, 104858.
- (12) Tsai, C.-M.; et al. Control of Crystal Structures and Optical Properties with Hybrid Formamidinium and 2-hydroxyethylammonium Cations for Mesoscopic Carbon-electrode Tin-based Perovskite Solar Cells. *ACS Energy Lett.* **2018**, *3* (9), 2077–2085.
- (13) Kamarudin, M. A.; et al. Suppression of Defect and Trap Density through Dimethylammonium-Substituted Tin Perovskite Solar Cells. *ACS Mater. Lett.* **2022**, *4* (9), 1855–1862.
- (14) Jokar, E.; et al. Mixing of Azetidinium in Formamidinium Tin Triiodide Perovskite Solar Cells for Enhanced Photovoltaic Performance and High Stability in Air. *ChemSusChem* **2021**, *14* (20), 4415–4421.
- (15) Kuan, C.-H.; et al. Additive Engineering with Triple Cations and Bifunctional Sulfamic Acid for Tin Perovskite Solar Cells Attaining a PCE Value of 12.5% without Hysteresis. *ACS Energy Lett.* **2022**, *7* (12), 4436–4442.
- (16) Jokar, E.; et al. Robust Tin-based Perovskite Solar Cells with Hybrid Organic Cations to Attain Efficiency Approaching 10%. *Adv. Mater.* **2019**, *31* (2), 1804835.
- (17) Shahbazi, S.; et al. Realizing a Cosolvent System for Stable Tin-based Perovskite Solar Cells Using a Two-step Deposition Approach. *ACS Energy Lett.* **2020**, *5* (8), 2508–2511.
- (18) Liu, X.; et al. Lead-Free Perovskite Solar Cells with Over 10% Efficiency and Size 1 cm² Enabled by Solvent–Crystallization Regulation in a Two-Step Deposition Method. *ACS Energy Lett.* **2022**, *7* (1), 425–431.
- (19) Song, D.; et al. Interfacial Engineering with A Hole-selective Self-assembled Monolayer for Tin Perovskite Solar Cells via A Two-step Fabrication. *ACS Energy Lett.* **2021**, *6* (12), 4179–4186.
- (20) Kuan, C.-H.; et al. How Can A Hydrophobic Polymer PTAA Serve as A Hole-transport Layer for An Inverted Tin Perovskite Solar Cell? *Chem. Eng. J.* **2022**, *450*, 138037.
- (21) Afraj, S. N.; et al. Quinoxaline-Based X-Shaped Sensitizers as Self-Assembled Monolayer for Tin Perovskite Solar cells. *Adv. Funct. Mater.* **2023**, *33*, 2213939.
- (22) Kuan, C. H.; et al. Dopant-Free Pyrrolopyrrole-based (PPr) Polymeric Hole-Transporting Materials for Efficient Tin-based Perovskite Solar Cells with Stability over 6000 h. *Adv. Mater.* **2023**, *35*, No. 2300681, DOI: [10.1002/adma.202300681](https://doi.org/10.1002/adma.202300681).